STUDIA UBB CHEMIA, LXVI, 1, 2021 (p. 73-88)
(RECOMMENDED CITATION)
DOI:10.24193/subbchem.2021.1.06

ALUMINUM PILLARED BENTONITE – CHARACTERIZATION AND SYNTHESIS OPTIMIZATION BY RESPONSE SURFACE METHODOLOGY

GABRIELA MUNTIANU[a*], ANDREI-IONUȚ SIMION[a*], CRISTINA-GABRIELA GRIGORAȘ[a], NICOLETA PLATON[a], ILEANA-DENISA NISTOR[a], GHEORGHIŢA JINESCU[b]

ABSTRACT. Bentonite is a clay mineral whose chemical structure can be easily modified by pillaring process for introduction of various cations such as aluminum, chromium, nickel, zinc etc. fact that conducts to attractive and versatile products suitable for diverse applications going from gas separation to pollutants removal or excipients for food industry for example.

This paper deals with the synthesis of aluminum pillared bentonite based on a process involving bentonite suspension and pillaring agent preparation, bentonite intercalation and calcination. The raw material and the obtained products were analyzed by X-ray diffraction, nitrogen adsorption-desorption technique, ammonia-temperature programmed desorption and scanning electronic microscopy. Three ratios of aluminum cations – amount of bentonite (5 mmol/g, 12.5 mmol/g, 20 mmol/g) and three calcination temperatures (300 °C, 400 °C, 500 °C) were used according to a Response Surface Methodology program aiming to attain the highest interlamellar distance, specific surface area and surface acidity. Collected data were fitted to second order polynomial equations. An aluminum cation – bentonite amount ratio of 12.5 mmol/g and a calcination temperature of 400 °C were found as appropriate conditions for bentonite pillaring process. Tests conducted on these settings showed that mathematical models were in good agreement with the experimental values presenting a high degree of accuracy.

Keywords: *bentonite, mathematical modelling, pillared clay, Response Surface Methodology*

[a] *"Vasile Alecsandri" University of Bacau, Department of Chemical and Food Engineering, 157 Calea Marasesti, 600115, Bacau, Romania*

[b] *Politehnica University of Bucharest, Department of Chemical and Biochemical Engineering, 1-7 Polizu, 011061, Bucharest, Romania*

**Corresponding authors: muntianu.gabriela@ub.ro, asimion@ub.ro*

INTRODUCTION

Clays are common natural minerals which, due to their specific properties [1, 2], are valuable in chemicals, pharmaceuticals, medical, cosmetics, ceramics, foods, agriculture or mining industries being used as catalysts [3], as drug carriers, gene vehicles [4], active ingredients or excipients [5], as intelligent food nanopackaging materials [6], as binding or dispersing agents, for clarification, deodorizing, neutralization and purification of petroleum products, removal of fats [7, 8] etc.

With layers consisting of one Al^{3+} octahedral sheet placed between two Si^{4+} tetrahedral sheets [9] and having montmorillonite as major constituent, raw bentonite is one of the most abundant 2:1 type clay minerals [10]. Depending on the more frequent encountered cation of crystal lattice, this material can be classified as sodium bentonite or as calcium bentonite [11]. It possesses high porosity, high specific surface, important hydration and swelling capacities, adsorption and ion exchange capacity etc. which make it suitable especially as adsorbent material for removal organic or inorganic polluting substances such as heavy metals [12, 13], dyes [14-16], chemicals [17, 18] etc. from wastewater, air or soil.

Bentonite adsorption capacity is based on two different mechanisms: *i)* an ion exchange reaction at permanent charged sites and *ii)* formation of complexes with surface hydroxyl groups [10, 19] and it can be enhanced by pillaring processes [9] which increase the basal spacing and adsorption surface area leading to more numerous active sites dispersed on the product surface [20].

The methods to modify the internal bentonite structure by pillaring in order to obtain three-dimensional microporous materials while maintaining the same thermal stable structure include: chemical modification (activation with mineral acids [21-23], alkaline activation, ion exchange etc.), physical modification (mechanic ways of operating on particle size), or thermal modification (also called thermal activation). The mentioned methods can be applied alone or in different combinations [24-26].

Final properties of the modified bentonite can be influenced by the selection of various work parameters. One of them is represented by the choice of cations used for pillaring process. Simple cations namely aluminum [25-29], iron, chromium [30, 31], nickel, zinc, magnesium, titan, copper, gallium [28, 30, 32, 33] and mixed cations such as aluminum – iron [31, 34], aluminum – chromium, aluminum – zirconium, aluminum – gallium [30, 33], aluminum – lanthanum – cerium, chromium – iron – zirconium or inorganic / organic compounds [32, 35] are successfully employed for this purpose.

The ratio of hydroxyl groups – metal (responsible for the material alkalinity) and the amount of cations reported at bentonite mass (metal/clay ratio) affect also the pillaring due to the fact that they control the *p*H value and the nature of cations species [32-34].

The final and the more important part of bentonite pillaring process is the thermal treatment achieved by calcination step to form fixed metal oxide pillars [35].

In this context, in the present paper, an experimental program was developed using different variations for two of the sodium bentonite pillaring process main parameters: aluminum cations – bentonite amount ratio and calcination temperature. The Response Surface Methodology was employed to establish the appropriate values of these parameters in order to achieve high basal spacing (also called interlamellar distance), an important specific surface area and a good surface acidity.

The raw material and the aluminum pillared bentonite were analyzed by X-ray diffraction, nitrogen adsorption-desorption technique, ammonia-temperature programmed desorption technique and by scanning electronic microscopy the registered results revealing that the obtained products possess properties making them suitable for various purposes (adsorption or catalysis being only two of them).

RESULTS AND DISCUSSION

Sodium bentonite and Al-PILCs characterization

X-ray diffractograms for sodium bentonite and for obtained aluminum pillared bentonites shown in Figure 1 reveal major changes in raw material structure after pillaring.

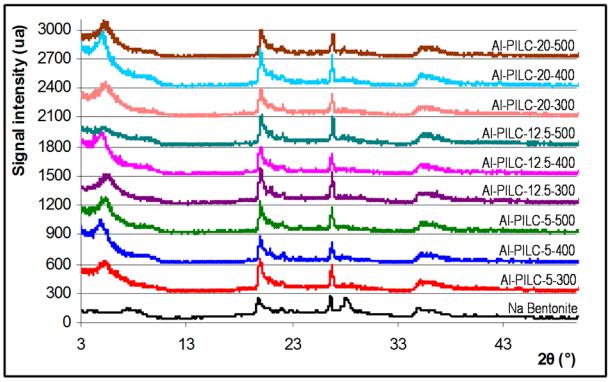

Figure 1. XRD patterns of sodium and Al-PILCs

With the help of Bragg's law applied on XRD data, the interlamellar distance was calculated for each pillared bentonite. According to values presented in Table 1, Al-PILCs obtained after calcination at 300 °C (Al-PILC-5-300, Al-PILC-12.5-300, Al-PILC-20-300) have low ID values of 1.65 – 1.7 nm which can be due to the fact that, at this temperature, the oxido-metallic pillars are not completely formed. The highest basal spacing (1.78 – 1.79 nm) was recorded for samples treated at 400 °C (Al-PILC-5-400, Al-PILC-12.5-400, Al-PILC-20-400). In these cases, the d_{001} peaks are relatively uniform which signifies that the pillaring process took place and led to rigid and homogeneous distributed pillars. At the temperature of 500 °C, aluminum pillared bentonite samples (Al-PILC-5-500, Al-PILC-12.5-500, Al-PILC-20-500) presented also lower ID values (1.66 – 1.67 nm). Moreover, characteristic peaks for pillared bentonite disappeared and the obtained products had tendencies to become amorphous.

Table 1. Experimental and predicted results obtained for Al-PILCs

Run	***Experimental code***	***ID [nm] (Mean ± Standard Deviation)***	
		Experimental results	***Predicted results***
1	Al-PILC-5-300	1.65 ± 0.0058	1.64
2	Al-PILC-5-400	1.78 ± 0.0076	1.79
3	Al-PILC-5-500	1.67 ± 0.0153	1.68
4	Al-PILC-12.5-300	1.64 ± 0.0321	1.65
5	Al-PILC-12.5-400	1.79 ± 0.0473	1.79
6	Al-PILC-12.5-500	1.70 ± 0.0153	1.69
7	Al-PILC-20-300	1.63 ± 0.0173	1.63
8	Al-PILC-20-400	1.78 ± 0.0100	1.77
9	Al-PILC-20-500	1.66 ± 0.0503	1.67

Run	***Experimental code***	***S^{BET} [m^2/g] (Mean ± Standard Deviation)***	
		Experimental results	***Predicted results***
1	Al-PILC-5-300	100.12 ± 0.5460	95.39
2	Al-PILC-5-400	129.05 ± 0.0289	134.62
3	Al-PILC-5-500	102.23 ± 0.7312	101.39
4	Al-PILC-12.5-300	104.63 ± 0.5056	111.17
5	Al-PILC-12.5-400	146.30 ± 0.6807	140.98
6	Al-PILC-12.5-500	99.55 ± 0.5008	98.33
7	Al-PILC-20-300	133.97 ± 0.5600	132.16
8	Al-PILC-20-400	152.80 ± 0.5292	152.55
9	Al-PILC-20-500	98.40 ± 0.2309	100.47

Run	***Experimental code***	***SA [mmol H^+/g] (Mean ± Standard Deviation)***	
		Experimental results	***Predicted results***
1	Al-PILC-5-300	0.339 ± 0.0055	0.348
2	Al-PILC-5-400	0.406 ± 0.0561	0.401
3	Al-PILC-5-500	0.222 ± 0.0053	0.218
4	Al-PILC-12.5-300	0.384 ± 0.0035	0.374
5	Al-PILC-12.5-400	0.437 ± 0.0051	0.431
6	Al-PILC-12.5-500	0.236 ± 0.0081	0.252
7	Al-PILC-20-300	0.390 ± 0.0058	0.391
8	Al-PILC-20-400	0.443 ± 0.0051	0.454
9	Al-PILC-20-500	0.291 ± 0.0061	0.279

Our data are consistent with those reported by Xu *et al.* [20] and by Gil *et al.* [36]. They show that when a temperature of 200-300 °C is used, the polycations are dehydrated. At temperatures between 300 °C and 600 °C, the polycations are dehydroxylated and the obtained materials possess a microporous [37] and rigid structure provided by formed oxido-metallic pillars separating adjacent silicate arrangements and thus increasing the distance between the bentonite layers. Chae *et al.* [38] stipulate that at higher temperatures (more than 700 °C), the resulted pillared products are progressively and irreversibly degraded and they cannot be used for retention processes.

Textural characteristics of sodium bentonite and Al-PILCs were determined by nitrogen adsorption/desorption isotherms at temperature of 350.45 °C. The results for raw material and for the three Al-PILCs having the highest interlamellar distances (Al-PILC-5-400, Al-PILC-12.5-400 and Al-PILC-20-400) are depicted in Figure 2. They were compared with the standardized forms proposed by International Union of Pure and Applied Chemistry (IUPAC) and they are similar type IV with H1 hysteresis this shape being encountered in materials that contain mainly mesoporous and small amounts of microporous particles. Between 0.02 and 0.03, the p/p_0 domain is occupied with nitrogen molecules. After the inflection point, the molecules adsorption is carried in mono molecular and poly molecular layers. Nitrogen capillary condensation begins in mesoporous zone and the hysteresis is evidenced in p/p_0 domain of 0.4 to 0.5. PILCs adsorption capacity fallows the sequence Al-PILC-20-400 > Al-PILC-12.5-400 > Al-PILC-5-400 being considerably greater than that of the natural bentonite.

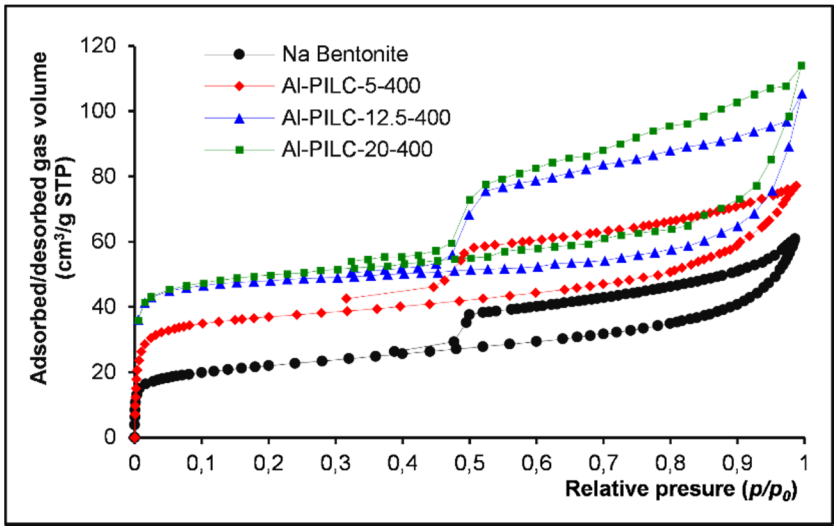

Figure 2. Nitrogen adsorption-desorption isotherms of raw and pillared sodium bentonite

From data summarized in Table 1, a significant S^{BET} amplification can be remarked compared to that of sodium bentonite which was of 31.1 m^2/g. When an aluminum cations – bentonite amount ratio of 5 mmol/g was used for pillaring process, the Al-PILCs specific surface areas were the lowest ones (100.12 m^2/g for Al-PILC-5-300) while the increase of this ratio to 12.5 mmol/g or to 20 mmol/g led to important S^{BET} augmentation (more than 146.30 m^2/g for Al-PILC-12.5-400 and more than 152.80 m^2/g for Al-PILC-20-400). In terms of calcination, the obtained results are consisting with the idea that the appropriate temperature for sodium bentonite pillaring process is of 400 °C since the best specific surface area (of 152.80 m^2/g) was registered for Al-PILC-20-400.

Beside to the high porosity, the prepared PILCs possess also an intensified surface acidity due to bentonite structure modification by the aluminum oxide pillars. Acid centers interact with ammonia in order to form NH_4^+ ions which fixe to the bentonite surface leading to a SA going from 0.222 mmol H^+/g for Al-PILC-5-500 to a least double one (0.443 mmol H^+/g for Al-PILC-20-400) of that recorded for initial sodium bentonite (0.180 mmol H^+/g).

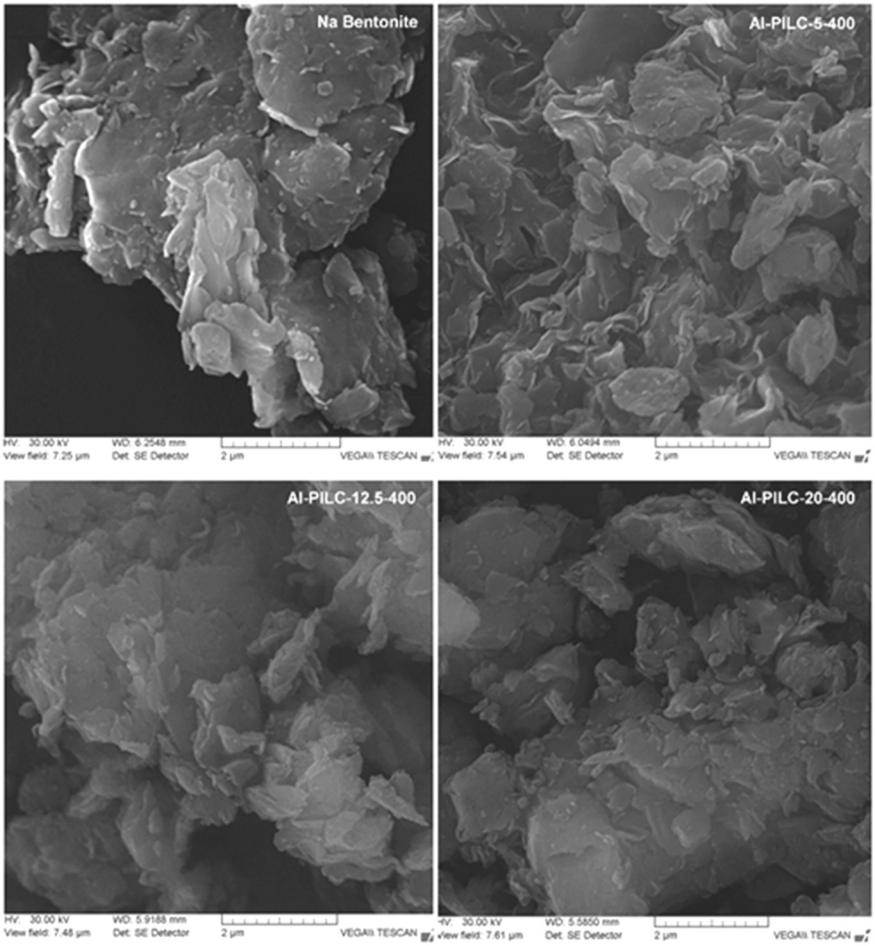

Figure 3. SEM micrographs of raw sodium bentonite and pillared materials

Similar results were emphasized also by other researches. Aluminum cations in pillaring agent insures higher molecular weight species that provide hydrothermal stability of pillared clays [39]. The nature of pillaring agent strongly depends of OH/metal ratio ($0.5 < OH/Al^{+3} < 2.5$) affecting the micropore volume and the surface area of pillared clay [37]. The Al^{+3}/g clay ratio plays a determinant role in the future properties of the obtained materials. For 30 and 90 mmol Al^{+3}/g clay the microporosity increases. At a Al^{+3}/g clay ratio of 180 mmol, an excess of aluminum oxide is introduced between the clay layers and, in spite, of a large distance, the micropore volume and area decreased [40].

Regarding the materials morphology, SEM images illustrated in Figure 3 show a clear evolution caused by the pillaring process.

The initial sodium bentonite presents a stratified, lamellar structure with visible layers mixed with big aggregates while in Al-PILCs products, the morphology is changed due to the aluminum greater amounts. The particles are smaller, finer and clearer and tend to form aggregates with a porous structure. These findings can be explained by the fact that the physio-chemical properties including microporosity of pillared clay increased with aging time of the pillaring solution due to the transformation of Al_{13} into $Al_{24}O_{72}$ (Al_{13} dimer) and other polynuclear cations [37, 41, 42]. It can be applied both for pillaring agent and for intercalated bentonite and consists of letting the reaction media to rest in a dark place at temperatures between 15 °C and 90 °C for periods going from one hour to one week in which the pillaring agent reacts with solution anions by hydrolysis, polymerization and complexation.

The obtained Al-PILCs structure sustains the possibility of materials ability to retain different molecules between their layers insuring by consequence the possibility to use them to different purposes one of them being as pollutants adsorbents.

Experimental design and optimization

Based on the experimental data and with the help of Expert Design 7.0 software, the obtained second order polynomial equations for three studied functions (ID, S^{BET}, SA) as affected by aluminum cations – bentonite amount ratio and calcination temperature parameters are presented below.

$$ID = 1.79 - 0.0058 \cdot A + 0.018 \cdot B + 0.0025 \cdot A \cdot B - 0.014 \cdot A^2 - 0.13 \cdot B^2 \quad (1)$$

$$S^{BET} = 140.98 + 8.96 \cdot A - 6.42 \cdot B - 9.42 \cdot A \cdot B + 2.60 \cdot A^2 - 36.23 \cdot B^2 \quad (2)$$

$$SA = 0.43 + 0.026 \cdot A - 0.061 \cdot B + 0.0045 \cdot A \cdot B - 0.0038 \cdot A^2 - 0.12 \cdot B^2 \quad (3)$$

In equations 1-3, the negative and positive signs of the coefficients indicate the effect of the studied parameters on the considered response.

Table 2 synthesizes the results of the quadratic model fitting in the form of analysis of variance (ANOVA).

Table 2. ANOVA for response surface quadratic models

Statistical parameter	***Response functions***		
	ID	S^{BET}	*SA*
p-value	0.0054	0.0054	0.0057
F-value	42.8742	16.6318	41.5201
Determination coefficient (R^2)	0.98619	0.96518	0.98575
Adjusted determination coefficient (Adj-R^2)	0.96319	0.90714	0.96201
Predicted determination coefficient (Pred. Adj. R^2)	0.83774	0.65388	0.83281
Coefficient of variation (CV), %	0.74854	5.64396	4.62402
Adequate Precision	16.11585	10.46069	17.85821
Predicted residual error sum of squares (PRESS)	0.00571	1335.27637	0.00921

The *p*-values inferior of 0.05 point out that the models terms are significant. The calculated *F*-values for the regressions were much greater than the values from Fisher tables ($F_{5, 3}$ = 9.01, for a 95% confidence level), confirming that the models fit to the experimental data. For all the established equations, there are only reduced chances that *F*-values this large could occur due to noise.

The determination coefficients R^2 of the quadratic regression models were close to unit indicating how much of the variability in data can be explained by the mathematical equations. The adjusted determination coefficient (Adj-R^2) which measures also the models goodness of fit has values were close to the corresponding determination coefficients values. The predicted determination coefficients for all the studied response functions are in reasonable agreement with the Adj-R^2.

At the same time, the low values of the coefficients of variation imply that the variation in the mean values were acceptable. Furthermore, adequate precision measures the signal to noise ratio and a ratio greater than 4 is generally desirable and designate satisfactory signals for the models to be used to navigate the design space.

The predicted residual sum of squares (PRESS) cross-validation technique identifies the model with better prediction. Its lower values sustain this hypothesis for ID and SA response functions. The high PRESS for S^{BET} could be explained by the fact that the model does not fit very well the edges of the studied domain. For example, if the experimental data recorded for Al-PILC-5-300 is ignored in the model generation process, the PRESS descends to 365.20846. In the same time, better results can be obtained for R^2 (0.99442), Adj-R^2 (0.98048), Pred. Adj. R^2 (0.89491) and for coefficient of variation (2.57534 %). Nonetheless, since in both cases, the calculated

relative error between the experimental data and those generated by the proposed equations is lower than 6 % for the Al-PILC-5-300 run, it can be considered that both the mathematical models express a good accuracy.

The three-dimensional response surface plots obtained from the RSM – CCD equations are illustrated in Figure 4. As it can be seen from this figure, both aluminum cations – bentonite amount ratio and calcination temperature affect the bentonite pillaring process. One can observe that an increase of the aluminum cations – bentonite amount ratio and of the calcination temperature from the 5 to 20 mmol/g and from 300 to 400 °C respectively impairs positively the values of the response functions while a temperature higher than 400 °C has a negative impact.

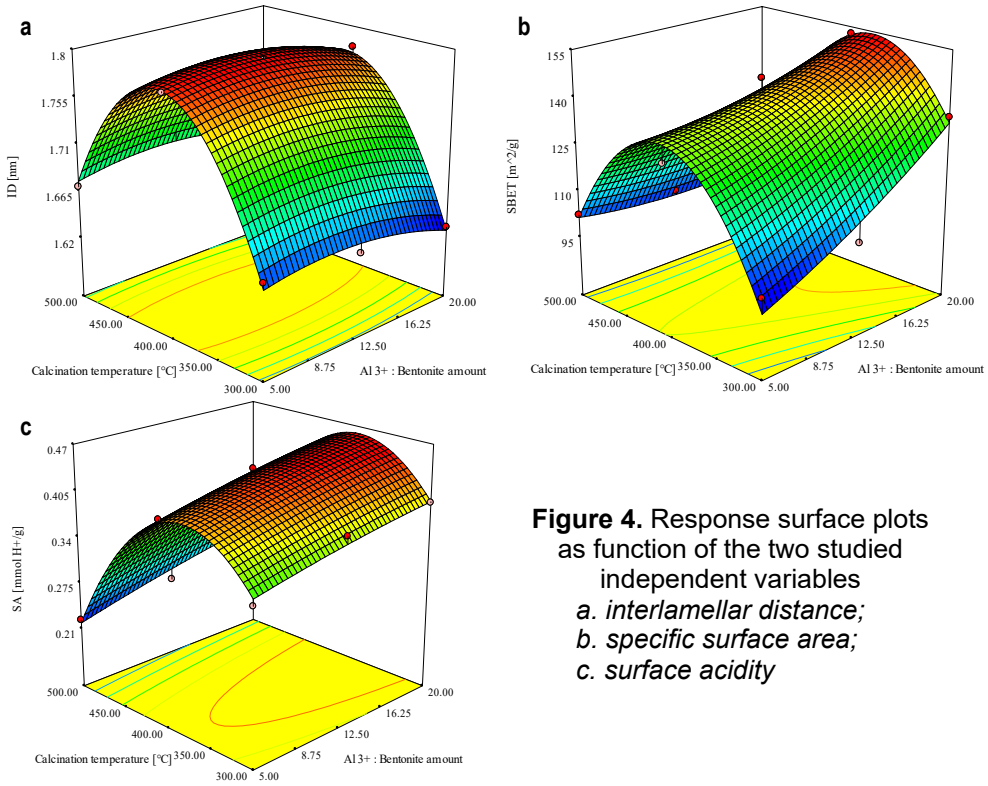

Figure 4. Response surface plots as function of the two studied independent variables
a. interlamellar distance;
b. specific surface area;
c. surface acidity

The developed mathematical models permitted to found the optimum values for the studied parameters as being 19.85 mmol/g for aluminum cations – bentonite amount ratio and 396.25 °C for the calcination temperature.

In these conditions, according to data furnished by the software, a maximum interlamellar distance of 1.77 nm, a specific surface area of 152.08 m^2/g and a surface acidity of 0.45 mmol/g H^+ could be obtained. Even though, while it is recommended to use a temperature of 400 °C for the calcination step, for aluminum cations – bentonite amount ratio a lower value of 12.5 mmol/g could be considered for two different reasons: firstly, because very similar values can be attained for the followed response functions and secondly, especially for economic causes. In this last case, the pillaring process is easier to handle because it implies the use of lower volumes of reagents and of prepared solutions and, in the same time, the entire procedure is less time and energy consuming.

Several experiments were carried using the stipulated optimal factors. The results (1.8 ± 0.0152 nm for ID; 145 ± 1.2678 m^2/g for S^{BET} and 0.439 ± 0.0032 mmol H^+/g for SA) revealed that the mathematical hypothesis is in a good agreement with the collected real data.

MATERIALS AND METHODS

Reagents

Hexahydrate aluminum chloride ($AlCl_3$ 6 H_2O), sodium hydroxide (NaOH) and silver nitrate ($AgNO_3$) involved as reagents in the experiments were of analytical grade and were purchased from PanReac AppliChem ITW Reagents (Germany), Lach-Ner (Czech Republic) and respectively from Chemical Company (Romania).

Sodium bentonite with a bulk density of 2400 kg/m^3, with 5 % humidity and particle size of 2 μm was supplied by Sigma Aldrich Romania and it was used as received, without purification and pretreatment.

In order to check their reproducibility, all the described analysis were carried out in triplicate and presented as mean values.

Sodium bentonite characterization

Sodium bentonite structure and interlamellar distance (ID) (d_{001}) were examined by X-ray diffraction (XRD) with a Siemens D5000 Diffractometer (Cu-K_α) (LabX, Canada) on a 2θ range between 3° and 50° with 0.02° step size using a 30 mA current and a 40 kV voltage.

Its adsorption/desorption isotherms and its specific surface area (S^{BET}) were determined by *Brunauer*, *Emmet* and *Teller* (BET) analysis performed with a Beckman Coulter SA 3100 Surface Area Analyser (Beckman Coulter GmbH, Germany). Prior to the analysis, the sample was degassed at 120 °C for 4 hours in order to eliminate any impurities and water traces. The studied gas was nitrogen of 99.9 % purity at a temperature of 350.45 °C.

Surface acidity (SA) was determinate by ammonia-temperature programmed desorption method. With the help of a gas carrier (nitrogen), ammonia vapors passed for 10 minutes through the aliquots of 0.2 g bentonite fixed bed. The sample was than repeatedly washed with nitrogen to remove the physiosorbed ammonia. Desorption step was carried out between 150 °C and 500 °C. The surface acidity was established as being the total ammonia amount desorbed per gram of bentonite.

Scanning electronic microscopy (SEM) analyses, realized with a Vega Tescan LSH II equipment (Tescan Orsay, France), was employed for sodium bentonite morphological characterization.

Aluminum pillared bentonite (Al-PILC) synthesis

For pillaring agent preparation, a 0.2 mol/L hexahydrate aluminum hydroxide solution was introduced in a Berzelius flask placed on a Nahita Blue 692 magnetic stirrer (Auxilab, Spain) set at 600 rpm, at room temperature. A 0.2 mol/L sodium hydroxide solution was added at constant flow of 1 mL/min in order to avoid aluminum hydroxide precipitation known as affecting the pillaring agent quality. The basicity relationship OH^-/Al^{+3} was maintained constant at a value of 2.2. The *p*H was adjusted at 4 with sodium hydroxide using a *p*H meter 315i Set (WTW, Germany).

A 2 % (w/w) bentonite suspension was prepared with distilled water and stirred for 2 hours at 800 rpm.

Resulted pillaring agent was added, drop by drop, at the same constant flow of 1 mL/min, into the bentonite suspension under agitation at 800 rpm, at room temperature. The obtained intercalated bentonite was let to rest for 12 hours for aging in a dark place and separated from the pillaring agent solution by simple decantation. The resulting bentonite slurry was repeatedly washed with distilled water. The removal efficiency of undesirable constituents was considered satisfactory when no precipitation was registered in the presence of silver nitrate.

The intercalated bentonite was then filtrated under vacuum and submitted to stabilization by drying at 120 °C for 4 hours in an Air Performance AP60 drying oven (Precisa, Romania) and calcinations for 2 hours at different temperatures using a Caloris L1003 laboratory furnace (Caloris Group, Romania).

Al-PILCs characterization

The obtained products were analyzed using the same methods and conditions as those specified for raw material characterization (see dedicated section previously presented).

Experimental design and optimization

The optimization of two of the main parameters influencing the bentonite pillaring process was conducted using a RSM costumed Central Composite Design (CCD). Design Expert 7.0 software was employed for experimental program setup, data analysis, mathematical model development and graph plotting. The different levels of variation tested are presented in Table 3.

Table 3. Experimental setup used for Al-PILCs

Run	*Experimental code*	*Aluminum cations - amount ratio*		*Calcination temperature*	
		Variation levels	*Real values [mmol/g]*	*Variation levels*	*Real values [°C]*
1	Al-PILC-5-300	- 1	5.0	- 1	300
2	Al-PILC-5-400	- 1	5.0	0	400
3	Al-PILC-5-500	- 1	5.0	1	500
4	Al-PILC-12.5-300	0	12.5	- 1	300
5	Al-PILC-12.5-400	0	12.5	0	400
6	Al-PILC-12.5-500	0	12.5	1	500
7	Al-PILC-20-300	1	20.0	- 1	300
8	Al-PILC-20-400	1	20.0	0	400
9	Al-PILC-20-500	1	20.0	1	500

Three studied response functions (interlamellar distance, specific surface area and surface acidity) were fitted with second order polynomial models expressed in the equation (4):

$$Y = a + b \cdot A + c \cdot B + d \cdot A \cdot B + e \cdot A^2 + f \cdot B^2 \quad (4)$$

where *Y* is the response function; *a* is the equation intercept, *b* and *c* are the linear coefficients, *d* is the cross-coefficient, *e* and *f* are the quadratic coefficients; *A* is the coded value for aluminum cations – bentonite amount ratio; *B* is the coded value for calcination temperature.

CONCLUSIONS

Sodium bentonite was used in this study as raw material for obtaining aluminum pillared materials. To this purpose, a process including bentonite suspension and pillaring agent preparation, bentonite intercalation and product stabilization was conducted in different experimental conditions.

Aluminum cations – bentonite amount ratio and calcination temperature were varied between 5 mmol/g and 20 mmol/g and between 300 °C and 500 °C according to a response surface methodology program. Both initial sodium bentonite and pillared clays were analyzed by X-ray diffraction, nitrogen adsorption-desorption technique, ammonia-temperature programmed desorption and scanning electronic microscopy and the resulted data were employed to develop mathematical models. A ratio of 12.5 mmol/g aluminum cations – bentonite amount and a calcination temperature of approximately 400 °C were found as appropriate for the clay pillaring process. In these conditions, the acquired interlamellar distance was of 1.79 nm, the specific surface area was of 146.3 m^2/g and the surface acidity attained 0.43 mmol H^+/g all the followed response functions having values considerable higher than those of the used raw material indicating that the established models were accurate presenting high confidence levels.

REFERENCES

1. A.V. Ursu; G. Jinescu; F. Gros; I.D. Nistor; N.D. Miron; G. Lisa; M. Silion; G. Djelveh; A. Azzouz; *J. Therm. Anal. Calorim.*, **2011**, *106(3)*, 965-971.
2. F. Rouquerol; J. Rouquerol; K. Sing; *Adsorption by powders and porous solids. Principles, methodology and applications,* Academic Press, London, **1999**, pp. 357-378.
3. R.A. Schoonheydt; *Appl. Clay Sci.*, **2016**, *131*, 107-112.
4. C.H. Zhou; L.Z. Zhao; A.Q. Wang; T.H. Chen; H.P. He; *Appl. Clay Sci.*, **2016**, *119*, 3-7.
5. P.S.C. Silva; S.M.B. Oliveira; L. Farias; D.I.T. Fávaro; B.P. Mazzilli; *Appl. Clay Sci.*, **2011**, *52(1)*, 145-149.
6. T.J. Gutiérrez; A.G. Ponce; V.A. Alvarez; *Mater. Chem. Phys.*, **2017**, *194*, 283-292.
7. J. Konta; *Appl. Clay Sci.*, **1995**, *10(4)*, 275-335.
8. F.J. Galindo-Rosales; F.J. Rubio-Hernández; *Appl. Clay Sci.*, ***2006***, *33(2)*, 109-115.
9. L. Gu; J. Xu; L. Lv; B. Liu; H. Zhang; X. Yu; Z. Luo; *Desalination*, **2011**, *269(1)*, 206-213.
10. M. El Bouraie; A.A. Masoud; *App. Clay Sci.*, **2017**, *140*, 157-164.
11. Z. Vryzas; V.C. Kelessidis; L. Nalbantian; V. Zaspalis; D.I. Gerogiorgis; Y. Wubulikasimu; *Appl. Clay Sci.*, **2017**, *136*, 26-36.
12. M.K. Uddin; *Chem. Eng. J.*, **2017**, *308*, 438-462.
13. J.N. Putro; S.P. Santoso; S. Ismadji; Y.-H. Ju; *Microporous Mesoporous Mater.*, **2017**, *246*, 166-177.

14. I. Belbachir; B. Makhoukhi; *J. Taiwan Institute Chem. Eng.*, **75**, 2017, 105-111.
15. N. Belhouchat; H. Zaghouane-Boudiaf; C. Viseras; *Appl. Clay Sci.*, **2017**, ***135***, 9-15.
16. X. Liang; Y. Lu; Z. Li; C. Yang; C. Niu; X. Su; *Microporous Mesoporous Mater.*, **2017**, *241*, 107-114.
17. K. Styszko; K. Nosek; M. Motak; K. Bester; *C. R. Chim.*, **2015**, *18(10)*, 1134-1142.
18. J. Fan; W. Yang; A. Li; *React. Funct. Polym.*, **2011**, *71(10)*, 994-1000.
19. T. Ngulube; J.R. Gumbo; V. Masindi; A. Maity; *J. Environ. Manag.*, **2017**, *191*, 35-57.
20. T. Xu; Y. Liu; F. Ge; L. Liu; Ouyang, Y., *Appl. Surf. Sci.*, **2013**, *280*, 926-932.
21. A.V. Ursu; C. Jinescu; I.D. Nistor; V.A. Aruș; G. Isopencu; M.A. Mareș; *Rev. Chim.*, **2010**, *(61)12*, 1226-1230.
22. S. Nousir; V.A. Aruș; T.C. Shiao; N. Bouazizi; R. Roy; A. Azzouz; *Microporous and Mesoporous Mater.*, **2019**, *290*, DOI: 10.1016/j.micromeso.2019.109652.
23. F. Boudissa; D. Mirilă; V.A. Aruș; T. Terkmani; S. Semaan; M. Proulx; I.D. Nistor; R. Roy; A. Azzouz; *J. Hazard. Mater.*; **2019**, *364(15)*, 356-366.
24. R.A. Schoonheydt; T. Pinnavaia; G. Lagaly; N. Gangas; *Pure Appl. Chem.*, **1999**, *71(12)*, 2367-2371.
25. R.A. Schoonheyat; T. Pinnavia; G. Lagaly; N. Gangas; *Pure Appl. Chem.*, **1999**, *71*, 2367-2371.
26. S. Nousir; V.A. Aruș; T.C. Shiao; N. Bouazizi; R. Roy; A. Azzouz; *Microporous Mesoporous Mater.*, **2019**, *290*, 109652.
27. G. Muntianu; N. Platon; A. Mardaru; I.D. Nistor; N.D. Miron; G. Jinescu; *U.P.B. Sci. Bull., Series B*, **2015**, *77(3)*, 151-164.
28. D.C. Mirilă; M.Ș. Pîrvan; N. Platon; A.M. Georgescu; V. Zichil; I.D. Nistor; *Acta Chem. Iași*, **2018**, *26(2)*, 263-280.
29. R. Azzallou; R. Mamouni; Y. Riadi; M. El Haddad; Y. El Mouzdahir; R. Mahboub; A. Elmchaouri; S. Lazar; G. Guillaumet; *Rev. Chim.*, **2010**, *61(12)*, 1155-1157.
30. A.-M. Georgescu; G. Brabie; I.D. Nistor; C. Penot; F. Nardou; *J. Porous Mater.*, **2015**, *22(4),* 1009-1019.
31. D.C. Mirilă; M.S. Pârvan; A.M. Roșu; V. Zichil; I.D. Nistor: *Sci. St. Res. Chem. Chem. Eng. Biotechnol. Food Ind.*, **2018**, *19(1)*, 63-72.
32. M.L. Chavez-Garcia; L. De Pablo-Galan; M.P. Saucedo-Ramirez; *J. Mex. Chem. Soc.*, **2006**, *50(1)*, 36-41.
33. P. Cañizares; J.L. Valverde; M.R. Sun Kou; C.B. Molina; *Microporous Mesoporous Mater.*, **1999**, *29(3)*, 267-281.
34. J.T. Kloprogge; L.V. Duong; R.L. Frost; *Environ. Geol.*, **2005**, *47(7)*, 967-981.
35. S. Sivakumar; S.K. Ghosh; A.D. Damodaran; K.G.K. Warrier; *Mater. Lett.*, **1997**, *31(1)*, 113-118.
36. S. Vercauteren; J. Luyten; R. Leysen; E.F. Vansant; *J. Membr. Sci.*, **1996**, *119(1)*, 161-168.
37. A.A.G. Tomlinson; *J. Porous Mater.*, **1998**, *5(3)*, 259-274.
38. A. Gil; L.M. Gandía; *Chem. Eng. Sci.*, **2003**, *58(14)*, 3059-3075.

39. H.J. Chae; I.-S. Nam; S.W. Ham; S.B. Hong; *Catal. Today*, **2001**, *68(1)*, 31-40.
40. M.N. Timofeeva; S.T. Khankhasaeva; Y.A. Chesalov; S.V. Tsybulya; V.N. Panchenko; E.T. Dashinamzhilova; *Appl. Catal., B*, **2009**, *88(1)*, 127-134.
41. A. Gil; M. Montes; *Langmuir*, **1994**, *10(1)*, 291-297.
42. A.-M. Georgescu; F. Nardou; I.D. Nistor; *Sci. Study Res. Chem. Chem. Eng., Biotechnol., Food Ind.*, **2016**, *17(3)*, 261-269.